Development of GIS-based disaster assessment system to reduce flood risks in urbanized creeks

T.S. Cheong[a,]*, M.L.A. Felix[b], S.M. Jeong[b]

[a]*National Disaster Management Institute, Seoul City, South Korea*
Email: bangjaeman@korea.kr
[b]*Department of Civil and Environmental Engineering, Kongju National University, Chunan City, South Korea*

ABSTRACT

This study developed a disaster assessment system, which integrated flood inundation, risk analysis system, and a decision support system. The parameter representation of the model was selected through sensitivity analysis, used for automated parameter optimization of the model. The Bocheong watershed in South Korea was selected for this study. The results of the simulation were used for disaster assessments; estimated results were calculated basing from flood damages from historical flood disasters, GIS, population, and inundation results. Lastly, this study developed a user-support system to provide real-time meteorological and hydrological data to local government and disaster situation room in South Korea. From the results of the evaluation, the developed model in this study was proven to be more excellent than ModClark model. The application of this model was found superior for ungaged basin such as mountainous area and small creek basins.

Keywords: GIS; Disaster management; Flood; Urban; Creek; Climate change

1. Introduction

The increase of the global temperature causes frequent and intensified rainfall occurrences, inundating urbanized areas. The intensity of the inundation is primarily affected by both precipitation and drainage characteristics [1]. Predicted occurrence of regional tropical cyclones for the twenty-first century is likely to have increased intensity, larger peak winds, and heavier precipitations [2].

Asia is the top continent in the world with the highest number of disasters fatalities and people affected from year 1980 to 2004 [3]. In the case of South Korea, natural disasters are an aftermath of typhoon occurrences, heavy rain, and floods. The damages induced by flooding in creeks have not decreased despite the execution of disaster mitigation. From year 2002 to 2006, 38.6% of all river and creek floodings, occurred from creeks; especially, for year 2004, where the inundation damages for creeks were higher in comparison to both streams and rivers. As of 2009 to the present, several creeks in South Korea are continuously inundated [4]. The number of disaster

*Corresponding author.

preventive systems developed for creeks in South Korea is inadequate.

As of 2008, the total number of creeks in South Korea is 22,664 with a total length of 35,815 km [5]. The characteristics of creeks are different from streams or rivers. Creeks constitute the upstream part of a river basin; with streambeds typically comprised of bedrock, gravel, and sand; with relatively high water level and water vortex occurrences are caused by steep bed slopes and creek meanderings. Locally concentrated rainfall causes sudden water level increase as compared to streams and rivers, which have bigger flow capacities.

The vulnerability reduction strategies for urbanized creeks should be developed and properly implemented to mitigate flood risks. However, the establishment of appropriate preventive measures for creeks is complex, due to diverging condition of creeks in various locations. The re-evaluation of risks should be performed to develop appropriate preventive measures to mitigate the inevitable effects of flooding, through disaster preparedness.

Various research and development (R&D) aims for the establishment of hasty restoration methods. However, the main purpose of this system is to accurately predict and forecast the anticipated occurrence of flooding disasters, to carry-out the necessary actions [6]. The need for a disaster preventive system, based on effective and accurate prediction and evaluations of flood inundations and real-time warning issues, is necessary.

2. Purpose and scope of the study

This study developed a system, which is an integration of flood inundation model, risk analysis system, and a decision support system. The improvement of the previously developed GIS-based flood analysis model was applied to various basins to determine existing problems. Recognized problems can be resolved by the reduction of input data to achieve optimum efficiency. Parameters used were: interception, infiltration, evapotranspiration, saturated flow, overland flow, and channel flow; and were automatically calculated by the model. The parameter representation was selected through sensitivity analysis, which was also used for the development of a user-interface method with automated parameter optimization. For the verification of the model, the application of the improved model was compared with the application of the previously developed rainfall-runoff model known as spatial runoff assessment tool (SRAT) by National Disaster Management Institute. The SRAT

programmed by C# uses filing algorithm [7] combined gradient algorithm to remove the DEM errors. Furthermore, the application of the GIS-based distributed model to ungaged watershed was demonstrated to attest the superiority of the developed model. The spatio-temporal variability of the model was investigated through the use of observed data. For this study, the Bocheong creek watershed in South Korea was selected. The results of the simulation are relevant for disaster assessments; estimated results were calculated based from flood damages from historical flood disasters, GIS, population, and from the results of the inundation. Lastly, this study developed a user-support system to provide real-time meteorological and hydrological data to the local government and disaster situation room in South Korea.

3. Srat model

The Soil Conservation Service Curve Number (SCS-CN) method was developed and documented by the United States Department of Agriculture in 1954; and it has been widely used and modified since it was first developed [8,9]. SCS-CN is simple method, developed for ungaged watersheds, which accounts for most runoff producing watershed characteristics such as soil type, land use, surface condition, and antecedent moisture condition and written as:

$$\frac{P_n[t,(i,j)]}{P[t,(i,j)]} = \frac{F[t,(i,j)]}{HS[t,(i,j)]} \tag{1}$$

wherein the precipitation that reaches the ground at time t is divided to surface runoff volume $P_n[t,(i,j)]$ and infiltrated water volume $I[t,(i,j)]$; H is the calibration parameter assigned to each cell. The effective value of the infiltration storage capacity and the potential maximum retention of the soil were determined by curve number parameter selection:

$$S(i,j) = 25.4\left(\frac{1,000}{CN(i,j)} - 10\right) \tag{2}$$

where $CN(i,j)$ is the curve number, at given cell location. In the simulation of the runoff process, the intercepted precipitation is deducted from the total precipitation for infiltration and runoff production. Once the interception reservoir is full of water, exceeded rainfall on the ground will split into surface and sub-surface flow. The mass balance equation of the infiltration reservoir is written as:

$$\frac{dF[t,(i,j)]}{dt} = P[t,(i,j)]\left\{1 - \frac{F[t,(i,j)]}{S[t,(i,j)]}\right\}$$
$$- W[t,(i,j)] - E[t,(i,j)]. \tag{3}$$

where $W[t,(i,j)]$ is outflow from infiltration reservoir to the sub-surface river network through a linear discharge,

$$W[t,(i,j)] = \frac{F[t,(i,j)]}{H_s} \tag{4}$$

where H_s is a calibration parameter assumed, constant with respect to time and space; $E[t,(i,j)]$ is evapotranspiration, can either be a direct input by manual computation or estimated internally through a simplified equation derived from the radiation method [10] based on air temperature, topographic, geographic, and climatic information. For different types of land use, monthly crops coefficients are given [10,11], representing the vegetation state in an annual growth cycle. The actual $E[t,(i,j)]$ for actual land use was calculated by a linear function of temperature, at each time step t for cell coordinates (i,j), in such a way that it can be aggregated to monthly time steps or disaggregated to shorter time steps without dispensing the long term balance expressed as:

$$E[t,(i,j)] = a + bT[t,(i,j)]N(i)W_{ta}(i) \tag{5}$$

where a and b are regression coefficients; $T[t,(i,j)]$ is the observed temperature at time t; $N(i)$ is the monthly mean of the maximum number of daily hours of daytime of the ith month; and $W_{ta}(i)$ is dependent upon the monthly average temperature and elevation above the sea level. Doorenbos and Pruitt [12] gave a comprehensive database of $N(i)$ and $W_{ta}(i)$ for various climatic conditions and phonological status for initial, mid-season, and late-season stages.

In order to perform a continuous time simulation of the water fluxes among soil, vegetation, and atmosphere, modification of the curve number method [13] is used within SRAT. Governing the mass balance of the infiltration reservoir in Eq. (3) is solved with the use of the fourth order Runge–Kutta method. Surface and sub-surface flows are propagated towards the basin outlet by applying Muskingum–Cunge with variable parameters [14]. The latter was determined on the basis of the "matched diffusivity" concept [15,16]. Each cell receives water from its up-slope neighboring cells and discharges to down-slope neighboring cell. For cells with converging flows, the upstream inflow hydrograph was taken as the sum of outflow hydrographs of the contributing upslope cells. Distinction between hill slope rill and network channel is based
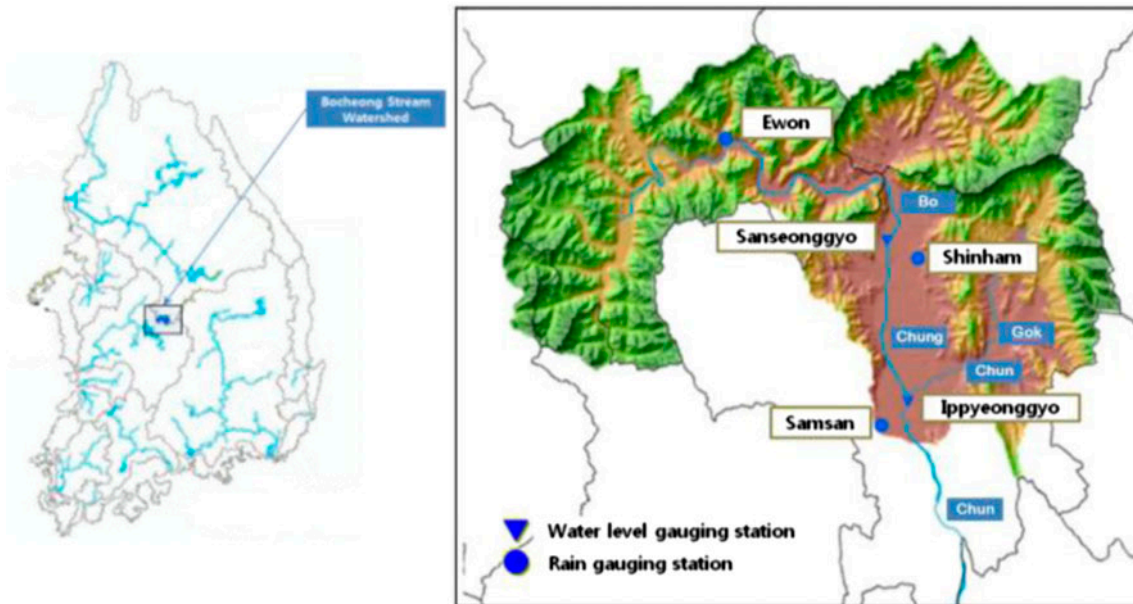

Fig. 1. Bocheong stream basin.

on the concept of "constant critical source area" [17]. The model considers evapotranspiration from soils and vegetation covers. The lateral sub-surface runoff and surface runoff from each hill slope cell are routed towards the basin outlet along the river network.

4. Model application

The Bocheong watershed is located at the central part of South Korea, with a 483.25 km^2 drainage area with a river length of 53.9 km. The main watershed and its tributaries has a total stream length of 735.25 km, an effective basin width (A/L) of 8.97 km; it is 28 km wide measured from the western to east direction and 33 km wide from northern to south direction. Majority of the watershed area are mountainous with a basin slope of 0.183. The altitudes EL. 220 m and EL. 600 m are the 50 and 90% of the watershed altitudes, respectively. Type-A soil type accounts for 47.9% of the total area, with high penetration; with a CN of 78.0 for AM-II. The watershed has a stream gradient of 1/172; with rapid upstream flow and calm downstream flow. The boundary of the watershed has the highest stream gradient due to its torrential configuration. Fig. 1 shows the location map of the Bocheong stream basin with the location of both water and rain-gaging stations.

The first process in the SRAT model is the land cover data segmentation. Segmentation process manages the constraint of region sizes to avoid over-sized objects. The relationship between objects (e.g. boundary length) is important for both runoff and ground flow routing. Both the stream network and watershed boundary were determined using DEM. Sink and flat areas from DEM data were removed. Filling and breaching algorithms were used for sink removal; and Jenson and Domingue algorithm, relief algorithm, and combined gradient algorithm were used to determine flow directions in flat area.

After segmentation and the construction of neighboring object relationships, the model imports precipitation, DEM, land cover, and soil properties. The SRAT model utilizes a lookup table between land cover types and properties [18] to derive parameters, such as Manning's coefficient for specific land covers [19]. Parameters of the SRAT were automatically calibrated. The values of the constant critical source area, A_0 were determined by comparing the stream network with the actual stream network extracted from soil map. The values of maximum Strickler roughness for the channel network, K_{sr}^0 and minimum Strickler roughness for the channel network, K_{sr}^1 were determined from the inversed value of Manning's roughness coefficient, calibrated with simulated

discharges, and measured data. The values of the channel width/height ratio for channel network, W_r, the channel width/height ratio for hillslope, W_v, the multiplying parameter for the interception reservoir, C_{int} and other parameters were verified and calibrated through the comparison of the observed and the simulated values, from auto-calibration method shown in Fig. 2. The simulated outflow discharge was compared with measured data from Bocheong Stream Basin to test sensitivity of parameters. The sensitivity analysis results of peak discharges with each parameter are shown in Table 1.

in which, B_p is the width of the rectangular cross-section of the sub-surface water flow, H_s is the bottom discharge parameter for the infiltration reservoir capacity, and H is the multiplying parameter for infiltration reservoir capacity.

For the auto-calibration of each parameter, sensitivity analysis was evaluated by the SRAT model. Parameter variation of the peak discharge, time to peak, and total runoff volume were also compared,
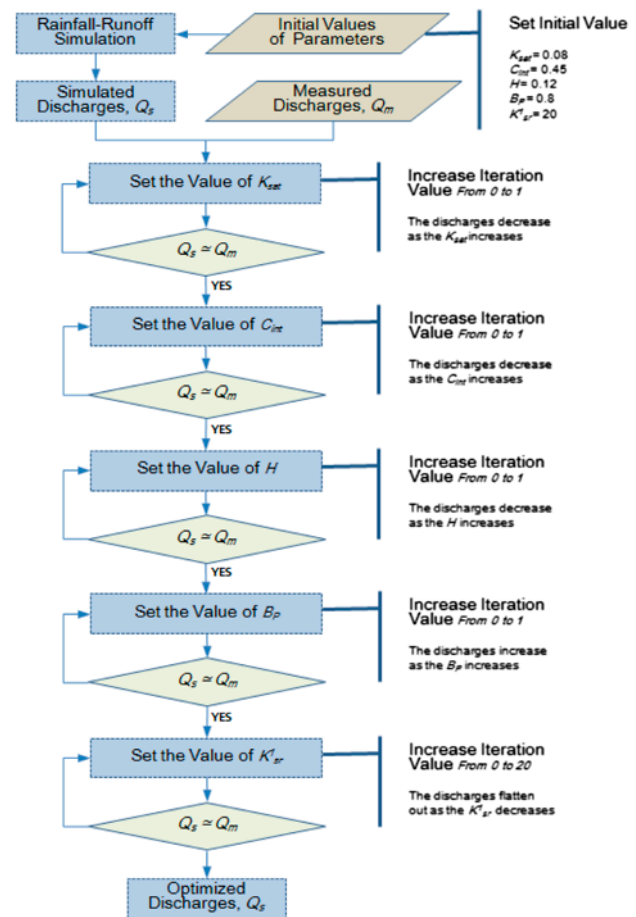

Fig. 2. Flowchart of parameter optimization method.

Table 1
Sensitivity results of parameters with the simulated discharges results

| Parameters | Sensitivity | | | | Ranges | |
	Large	Middle	Small	No sensitivity	Optimal	Default
A_0 (km^2)		○			0.25–1	0–100
W_v				○	–	0–1,000,000
W_r		○			5–25	0–100
K_{sr}^0			○		5–20	0–100
K_{sr}^1		○			10–40	0–100
K_{sat} (m/s)	○				0.05–0.25	0–1
B_p (m)		○			0.4–0.8	0–1
H_s	○				30,000–80,000	0–100,000
H	○				0.06–0.09	0–1
C_{int}			○		0.5–1	0–1

shown in Fig. 3. The minimum and maximum values were considered for the comparison of parameter sensitivity. Parameter variations were determined from the plus and minus 10% of the median values.

In the SRAT model, the optimal combination was quantitatively assessed using the root mean square error (RMSE), correlation coefficient (CC), Nash–Sutcliffe efficiency coefficient (EC), relative percentage error (RPE), mean absolute deviation (MAD), and relative average deviation (RAD). The RMSE is determined by:

$$\text{RMSE} = \sqrt{\sum e_i^2 / n} \tag{5}$$

where e_i is the difference of the observed and the forecasted values and n is the number of data. To determine the correlation between two parameters, x
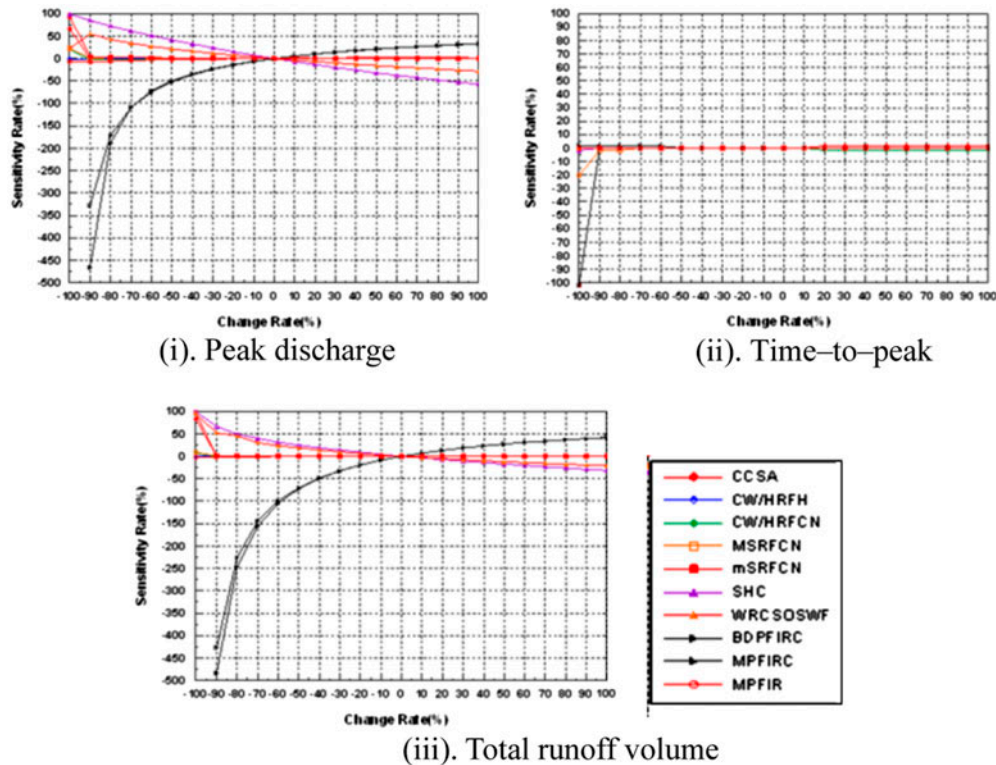

(i). Peak discharge

(ii). Time–to–peak

(iii). Total runoff volume

Fig. 3. Results of the sensitivity analysis.

and y, the coefficient of correlation was calculated with $SS/(SI \cdot SE)^{1/2}$; where SS is equal to the sum of squares of the deviation of x and y $(\sum (x_i - \bar{x})(y_i - \bar{y}))$; SI is the sum of squares of the deviation of $x(\sum(x_i - \bar{x})^2)$ and SE is the sum of squares of the deviation of $y(\sum(y_i - \bar{y})^2)$. The Nash–Sutcliffe EC quantitatively describes the accuracy of the simulated runoff with respect to the observed data by EC = (SE—SSE); where an efficiency of 1 means that the model perfectly matched the values of the observed data. RPE measures uncertainty of a measurement, relative to the size of the measurement written as, RPE $= |Q_P - \bar{Q}_P| / \bar{Q}_P \times 100(\%)$; where Q_P is the predicted peak discharge and $\bar{Q}_P$ is the observed peak discharge. The MAD is given as $\sum |y_i - \bar{y}|/n$. RAD is defined as the MAD divided by the sample mean (MAD/$\bar{y}$).

5. Results and discussion

In order to calibrate the SRAT model, the land use map and soil map were used as input data in the model. The slope of each 30×30 m grid of the Bocheong stream network was constructed by the use
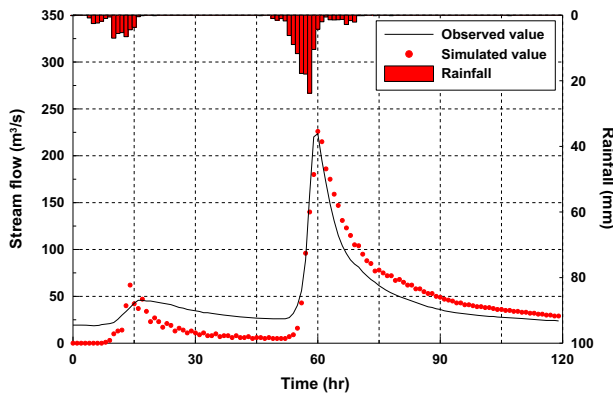

Fig. 4. Results of the simulation parameter calibration, at Ipyeonggyo water level gaging station, for the July 2005 event.
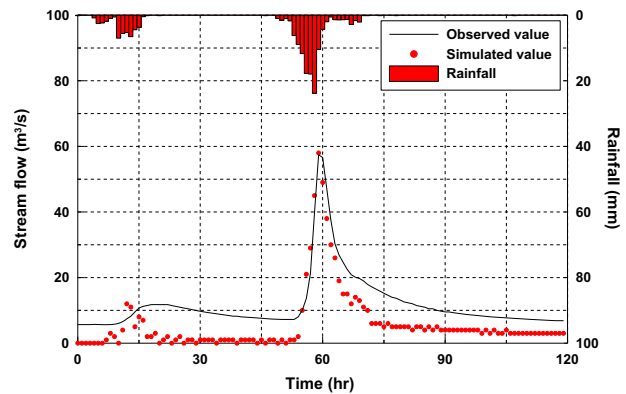

Fig. 5. Comparison between the observed value and the simulated results at Sanseonggyo water level gaging station for the July 2006 event.
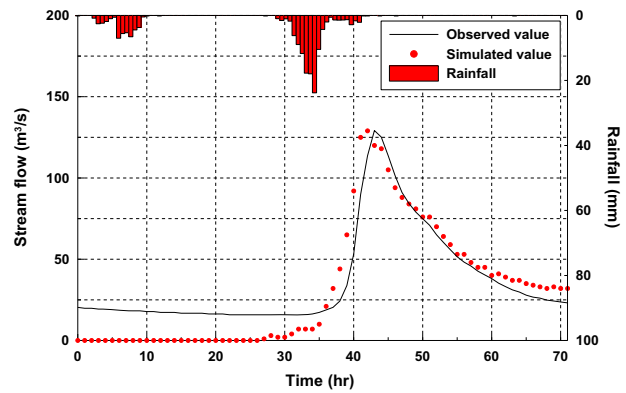

Fig. 6. Comparison between the observed value and the simulated results at Ipyeonggyo water level gaging station for the August 2007 event.

of SRAT model. Three rainfall events were selected for the simulation (i.e. July 2005, July 2006, and August 2007 events). In this study, the soil map and land use map were gathered from WAMIS. The topographic and meteorological input data constructed from year 2005 were used for calibration of the SRAT through the comparison of the observed and simulated values in the Ipyeonggyo water level

Table 2
Error values for the simulated results (July 2005)

Statistical error	Error values
RMSE	17.121
EC	0.801
MAD	16.039
RAD	0.348
CC	0.945
RPE	0.168

Table 3
Statistical errors of the simulated results

Statistical errors	Spatial transition	Temporal transition
RMSE	6.884	13.437
EC	0.399	0.762
MAD	6.494	12.229
RAD	0.550	0.339
CC	0.941	0.940
RPE	1.057	0.130

gaging station. Fig. 4 shows the runoff results after parameter calibration.

The observed data matches the results of the simulation; however, the peak flow value was underestimated. Also, the low flow and high flow were consistent and matching with the observed data.

The results of the simulation were quantitatively examined through the calculation of RMSE, EC, MAD, RAD, CC, and RPE. Table 2 summarizes the calculated error values by: RMSE with 17.121, NSEC with 0.801 m³/s and CC with 0.945, which suggests that the simulated and measured values showed good agreement.

The application of the model in ungaged small stream was assessed by reviewing the spatio-temporal parameter. Parameter optimization was reviewed with the July 2005 event to calibrate the parameter of the upstream basin located at Sanseonggyo water level gaging station through simulation. Fig. 5 shows results of the simulation and the observed values. It was observed that the low flow of simulated value, in comparison with the observed value, was underestimated while the peak flood occurrence was coinciding with the observed value.

For spatio-temporal parameter transitions of the SRAT model, the July 2006 event and the August 2007 events were used for additional rainfall-runoff simulations with the model already calibrated. The simulation of parameter optimization was based on the July 2007 event for the Sanseonggyo station which was also compared with the results of the simulation. The verification of the spatio-temporal parameter with time occurrence was performed with the August 2007 flood event and as shown in Fig. 6.

The summary of quantitative review (i.e. RMSE, EC, MAD, RAD, CC, and RPE) for the spatial transition and temporal transition are shown in Table 3.

It is shown in Table 3 that the quantitative evaluation for the spatial transition parameter for: the RMSE was 6.884 m³/s; and CC with 0.941; the results of the simulation showed a good match with the observed value. While the simulated results of the temporal transition yielded to: RMSE 13.437 m³/s, Nash–Sutcliffe EC 0.762 and the CC 0.940; with these, the results of the simulation and the observed values were observed to be a good match.

For the comparison of models with the developed model, the events July 2005, July 2006, and August 2007 were used for the simulations. The observed values, the results of the simulation from the developed model and results of the simulation using the Mod-Clark model were graphed as shown in Fig. 7(i–iii) for the July 2005, July 2006, and August 2007 events, respectively.

The validation of the SRAT model was performed through the comparison of the results of the simulation from both the developed model and the ModClark model, and was compared with the observed data. Results of the simulation from the developed model and the overall runoff observed patterns showed to be fairly matched. Also, the occurrence of runoff and time-to-peak also showed good agreements with the observed values. However, the results of the simulation with ModClark in comparison to the observed values also showed good agreement, however, the overall runoff pattern showed
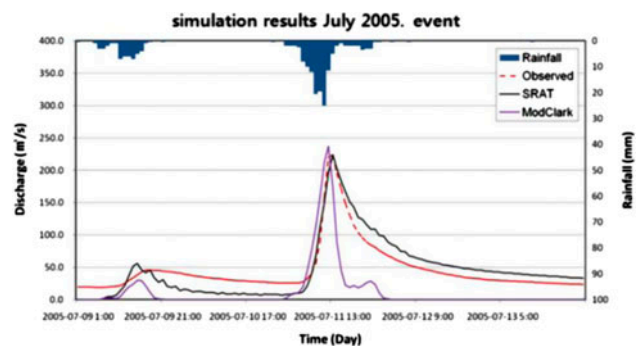
(i). Results of the simulation (July 2005 event)
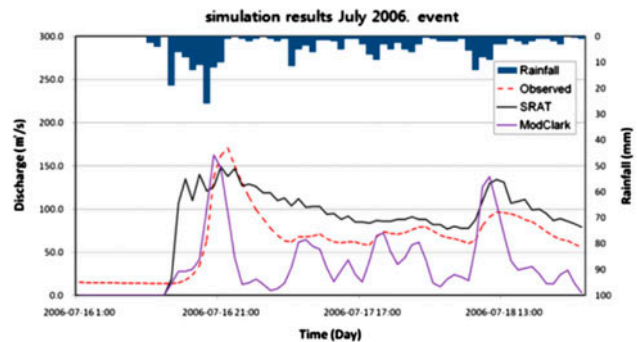
(ii). Results of the simulation (July 2006 event)
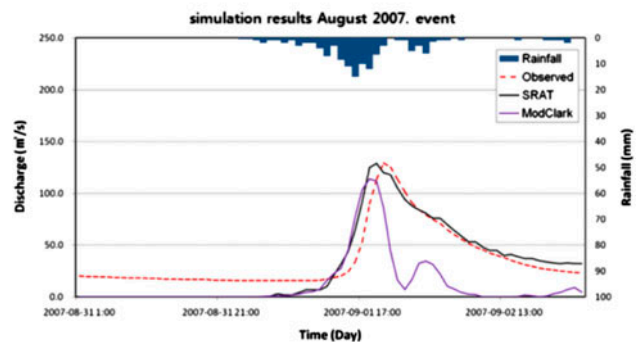
(iii). Results of the simulation (August 2007 event)

Fig. 7. Results of the simulation in comparison to the Mod-Clark Model.

Table 4
Results of the comparison between the Developed model and the ModClark model

Statistical error	July 2005		July 2006		August 2007	
	Developed model	ModClark model	Developed model	ModClark model	Developed model	ModClark model
RMSE	17.171	43.112	33.523	43.106	14.437	34.070
EC	0.801	−0.264	0.116	−0.461	0.762	−0.328
MAD	16.039	37.182	25.913	34.689	12.229	27.782
RAD	0.348	0.806	0.402	0.538	0.339	0.771
CC	0.945	0.731	0.778	0.610	0.940	0.616
RPE	0.168	5.982	12.769	4.748	0.130	11.897

extensive differences. The quantitative results are summarized in Table 4. It is shown that the developed model in this study showed superior performance as compared to the ModClark model.

6. Conclusions

The sensitivity analyses of the parameters (i.e. peak flow, peak flow time, and total flow) of the model were conducted for the automated parameter optimization of the system. Results of sensitivity analyses showed that highly sensitive parameters (i.e. saturated hydraulic conductivity, width of the rectangular cross section of the sub surface water flow, bottom discharge parameter for the infiltration reservoir capacity, and the Multiplying parameter for the interception reservoir).

In this study, the runoff simulation was conducted to examine and verify the applicability of the developed model to simulate accurate flood discharges for the Bocheong creek watershed. After the runoff simulation, parameter optimization was performed through the comparison of observed value with the simulated value.

Parameter optimization was conducted through the comparison of observed value of the flood event at Ippyeonggyo station and the flood event in Bocheong creek at July 2005. The examination of the spatio-temporal variability of the parameter was conducted after the simulation of parameter optimization for the Sanseonggyo station. And lastly, the additional simulations for the events July 2006 and August 2007 were also conducted for the examination of the temporal variability of the parameter. The result on the analysis of spatio-temporal variability of the parameter was confirmed from segmentalized sub-basin under a standard basin.

Previously developed models were compared with the developed model to demonstrate the superiority of the developed model. It was compared with a quasi-distributed model ModClark and HEC-HMS. The result of simulation was quantitatively evaluated through the use of statistical indicators. Results of the evaluation showed that the model developed in this study was proven to simulate more accurate flow discharges than the ModClark model.

The application of the developed model is superior for ungaged basin. The limitations of the developed model were primarily caused by minimal requirement of input data for model simulation (i.e. three topographic data – DEM, land use map, and soil map; and two meteorological data – rainfall and temperature).

References

[1] Intergovernmental Panel on Climate Change, IPCC, Managing the Risks of Extreme Events and Disasters to Advance Climate Change Adaptation. A Special Report of Working Groups I and II of the Intergovernmental Panel on Climate Change [C.B. Field, V. Barros, T.F. Stocker, D. Qin, D.J. Dokken, K.L. Ebi, M.D. Mastrandrea, K.J. Mach, G.-K. Plattner, S.K. Allen, M. Tignor, P.M. Midgley (eds.)], Cambridge University Press, Cambridge, UK, and New York, NY, USA, 2012. p. 582.

[2] Intergovernmental Panel on Climate Change, IPCC. AR4 WG2, M.L. Parry, O.F. Canziani, J.P. Palutikof, P.J. van der Linden, C.E. Hanson (ed.), Climate Change 2007, Impacts, Adaptation and Vulnerability, Contribution of Working Group II to the Fourth Assessment Report of the Intergovernmental Panel on Climate Change, Cambridge University Press, Cambridge, 2007.

[3] D. Stromberg, Natural disasters, economic development, and humanitarian aid, J. Econ. Perspect. 21(3) (2007) 199–222.

[4] National Emergency Management Agency, NEMA, Annual Disaster Assessment Report, South Korea, 2008.

[5] National Emergency Management Agency, NEMA, Development of regional safety assessment guideline to set up efficiency registration for flood insurance, South Korea, 2009.

[6] National Institute for Disaster Prevention, NIDP, Establishment of information supporting scheme and pilot test of small stream risk analysis system, National Institute for Disaster Prevention, Seoul, South Korea, 2011.

[7] S.K. Jenson, J.O. Domingue, Extracting topographic structure from digital elevation data for geographic information system analysis, Photogram. Eng. Remote Sens. 54(11) (1988) 1593–1600.

[8] R.H. McCuen, Hydrologic Analysis and Design, 3rd ed., Prentice Hall, Englewood Cliffs, 2003.

[9] S.K. Mishra, V.P. Singh, Soil Conservation Service Curve Number (SCS-CN) Methodology, Kluwer Academic, Dordrecht, 2003.

[10] J. Doorenbos, W.O. Pruitt, A. Aboukhaled, J. Damagnez, N.G. Dastane, C. Van der Berg, P.E. Rijtema, O.M. Ashford, M. Frere, Guidelines for predicting Crop Water Requirements, FAO Irrigation and Drainage Paper, Rome, 1984.

[11] D.R. Maidment (ed.), Handbook of Hydrology, McGraw-Hill, New York, NY, 1993.

[12] J. Doorenbos, W.O. Pruitt, Crop water requirements. FAO Irrigation and Drainage Paper No. 24, FAO, Rome, Italy, 1992.

[13] Soil Conservation Service, National Engineering Handbook, Section 4, Hydrology, US Department of Agriculture, Washington, DC 1972.

[14] J.A. Cunge, On the subject of a flood propagation computation method (Muskingum method), Hydraul. Res. 7 (1969) 205–230.

[15] V.M. Ponce, Diffusion wave modelling of catchment dynamics, J. Hydraul. Eng. ASCE 112(8) (1986) 716–727.

[16] S. Orlandini, R. Rosso, Diffusion wave modelling of distributed catchment dynamics, J. Hydrol. Eng. ASCE 1(3) (1996) 103–113.

[17] D.R. Montgomery, E. Foufoula-Georgiou, Channel network source representation using digital elevation models, Water Resour. Res. 29(12) (1993) 3925–3934.

[18] W.J. Rawls, L.R. Ahuja, D.L. Brakensiek, A. Shirmohammadi, Infiltration and soil water movement, Chap. 5, in: D.R. Maidment (Ed.), Handbook of Hydrology, McGraw-Hill, New York, NY, 1992, pp. 5.1–5.51.

[19] C.J. Sande, S.M. de Jong, A.P.J. de Roo, A segmentation and classification approach of IKONOS-2 imagery for land cover mapping to assist flood risk and flood damage assessment, Int. J. Appl. Earth Obs. Geoinf. 4 (2003) 217–229.